BUOYANCY HEAT TRANSFER IN STAGGERED DIVIDING SQUARE ENCLOSURE

by

Viktor I. TEREKHOV [a*], ***Alexander V. CHICHINDAEV*** [b], ***and Ali L. EKAID*** [a,b]

[a] Kutateladze Institute of Thermophysics SB RAS, Novosibirsk, Russia
[b] Novosibirsk State Technical University, Novosibirsk, Russia

Original scientific paper
UDC: 533.6.011:536.25:517.96
DOI: 10.2298/TSCI110109052T

This study represents the results of numerical simulation of fluid motion and free-convective heat transfer in a square cavity with partitions mounted on the lower (heated) and upper (cooled) walls. The height of partitions and their heat conductivity were varied K_r = 2-8000 together with Rayleigh number Ra = 10^3-10^6, which corresponded to the laminar flow. It is assumed that vertical walls of the cavity are adiabatic, and its horizontal walls are kept at constant, but different temperatures. The numerical solution based on transformation of determining equations by the method of finite differences was achieved. The obtained results show that the surface-average heat transfer coefficient decreases with a rise of partition height due to the suppression of convection. Also the results show that with an increase in heat conductivity coefficient of partitions, the Nusselt number increases significantly. In addition, it was found that when the value of relative heat conductivity coefficient changes by four orders, the Nusselt number for the highest partitions changes by the factor of 1.5-2 only and the integral heat transfer through the whole interlayer increases with development of the heat exchanging area.

Key words: *buoyancy heat transfer, staggered partitions, square enclosure*

Introduction

Recently natural convection in an enclosure with partial vertical divider has attracted the considerable interest. This interest stems from the significance of buoyancy-induced flows in various engineering and technological applications such as convective heat loss from solar collectors, thermal insulation, nuclear reactors, heat-recovery systems, energy conservation in buildings, air conditioning and ventilation, cooling of electronic equipments, and semiconductor production.

Many researchers have been studied the natural heat transfer and fluid flow in square enclosure with and without divided partitions to study the effect of partitions on the heat transfer mechanism inside the cavities [1-24]. Karayiannis *et al*. [1] have studied numerically convective heat transfer for air in rectangular cavities without a partition and with a vertical

* Corresponding author; e-mail: terekhov@itp.nsc.ru

partition with different constant temperatures on the opposite walls. The aspect ratio was changed from A = 0.1 to 16, and the Rayleigh number was changed from Ra = 10^5 to $1.6 \cdot 10^8$ with the partition thickness and thermal conductivity being varied, the Nussult number was reduced by 12% due to the partition. Yucel *et al.* [2] have studied natural convection in partially divided square enclosures with differentially heated lateral, adiabatic, and perfectly conductive horizontal walls. They have concluded that the mean Nusselt number decreases with increasing the height and number of partitions. Dagtekin *et al.* [3] have investigated natural convection heat transfer by heated partitions within an enclosure. They have found that as the partitions height increases, the mean Nusselt number increases and that the position of partitions has more effects on fluid flow than that of heat transfer. Nakhi *et al.* [4] studied the laminar natural convection flow of a viscous fluid in an inclined enclosure with partitions; the range of Rayleigh number and the angle of inclination was 10^3 to 10^6 and 0-90°, respectively. It was found that the average Nusselt number increases with an increase in the Rayleigh number. Also, as the dimensionless partition height increases, the flow speed within the partitioned enclosure decreases resulting in less wall heat transfer. In addition, it was found that the average Nusselt number decreases as the partitioned enclosure inclination angle increased beyond 30°. Nansteel *et al.* [5, 6] performed experiments on natural convection heat transfer in undivided and partially divided rectangular enclosures. In their studies, the vertical walls were maintained at different temperatures while the horizontal walls were adiabatic. The experiments were carried out with water for Rayleigh numbers over the range Ra = 10^{10}-10^{11}. The vertical partial partition was fitted on the top surface. The correlations for the average Nusselt number were generated for the cases of conducting and non-conducting partial divisions as a function of Rayleigh number and aperture ratio (the height of partition to the height of enclosure). It was shown that the partial divisions significantly decreased the total heat transfer, especially when the partitions were non-conducting. Lakhal *et. al.* [7] studied numerically natural convection in inclined rectangular enclosure with perfectly conducting fins attached to the heated wall. The parameters governing this problem are Rayleigh number Ra = 10^2-$2 \cdot 10^5$, aspect ratio A = 2.5-∞, and inclination angle φ = 0-60°. The results indicate that heat transfer through the cover is considerably effected by the presences of the fin. Also, at low Rayleigh numbers the heat transfer regime is conduction predominantly. The results show that the walls decrease significantly heat transfer through the layer by suppression of vortex motion inside the cavity. At the same time the thermal conductivity of ribs may strengthen heat transfer by increasing the surface area which is in contact with gas [8-16]. The authors of these works showed that heat transfer can be effectively controlled in wide ranges by changing the heights of the ribs, their number, and thermal conductivity. Mushatet [17] conducted a detailed numerical study of turbulent convection in a square cavity with two partitions of different heights, located on the lower wall. The complex scenarios of development of the flow, depending on location of partitions, their heights, and values of Rayleigh numbers were shown in this work. Analysis of published data showed some trends for development of free convection when having partitions in the layers. Depending on the thermal boundary conditions, locations of the ribs or blocks, their geometry and the coefficient of thermal conductivity can be got as increasing and decreasing average heat transfer. The problem is complex and has multiple factors; therefore many of its aspects have still remained unsolved. The data of many experimental and numerical researches testify natural convection heat transfer in the enclosures with partitions and ribs.

In the present study natural convection in a square cavity with partial checkerboard division on the upper and lower walls has been considered. It is supposed that the vertical sidewalls are adiabatic, and the horizontal top and bottom walls are kept at constant, but different temperatures. Partitions with finite thickness and thermal conductivity are mounted on the top and bottom cavity of the walls in a checkerboard pattern. Such geometry is typical for cooling electronics, as well as the processes of heat treatment and drying of various products. For different values of Rayleigh numbers and wall height freely convective gas flow and temperature fields inside the cavity are expected. Particular attention is paid to the analysis of local heat transfer, which characterizes the presence of the areas of high and low heat transfer to all elements which produce heat, as well as integral heat transfer through the cavity. These data may serve as a basis for optimizing study limits for the influence of installation of blocks on intensity of heat transfer processes.

The mathematical model

The physical domain considered in this study is a 2-D square enclosure with partially divided staggered partitions shown in fig. 1. The length of the side of the square is denoted by L. The thickness and length of partitions are represented by d and h, respectively. Physical and mathematical statement of the problem, boundary conditions and numerical method are described in detail in work [24].

Here we consider the steady laminar, 2-D, natural convective flow inside a partitioned enclosure. The temperatures T_h and T_c are uniformly imposed on two opposing horizontal walls such as $T_h > T_c$ while the other walls are assumed to be adiabatic. Figure 1 shows the schematic and co-ordinate system of the problem under consideration. The fluid is assumed to be incompressible, Newtonian, and viscous; it has constant thermophysical properties except the density in the buoyancy term of the momentum equations. The effect due to viscous dissipation is assumed to be negligible. The governing equations for this problem are based on the balance laws of mass, linear momentum, and energy. Taking into account the assumptions mentioned above, and applying the Boussinesq approximation for the body force terms in the momentum equations, the governing equations can be written in dimensionless stream function-vorticity form as:

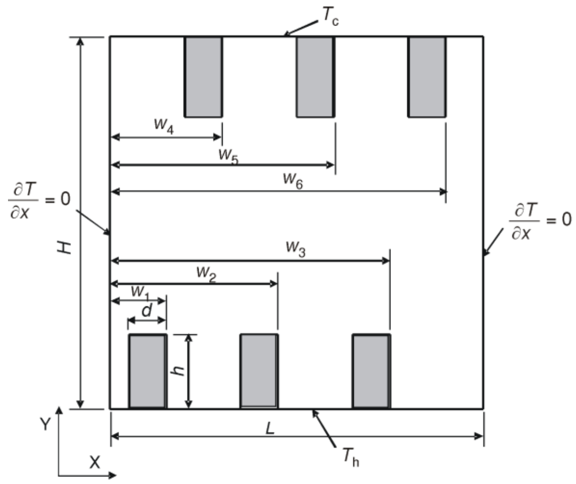

Figure 1. Problem schematic and co-ordinate system

$$U\frac{\partial \zeta}{\partial X} + V\frac{\partial \zeta}{\partial Y} = \Pr\left(\frac{\partial^2 \zeta}{\partial X^2} + \frac{\partial^2 \zeta}{\partial Y^2}\right) + \mathrm{Ra}\Pr\frac{\partial \theta}{\partial X} \tag{1}$$

$$\frac{\partial^2 \psi}{\partial X^2} + \frac{\partial^2 \psi}{\partial Y^2} = -\zeta \tag{2}$$

$$U\frac{\partial\theta}{\partial X}+V\frac{\partial\theta}{\partial Y}=\frac{\partial^2\theta}{\partial X^2}+\frac{\partial^2\theta}{\partial Y^2} \tag{3}$$

where the dimensionless stream function and vorticity are defined in the usual way as:

$$U=\frac{\partial\psi}{\partial Y},\quad V=-\frac{\partial\psi}{\partial X},\quad \zeta=\frac{\partial V}{\partial X}-\frac{\partial U}{\partial Y} \tag{4}$$

For the solid region (in the partitions), the energy equation for heat transfer by conduction, eq. (3), becomes:

$$\frac{\partial^2\theta}{\partial X^2}+\frac{\partial^2\theta}{\partial Y^2}=0 \tag{5}$$

The equality of thermal fluxes takes place on the interface between the solid and gas:

$$K_f\frac{\partial\theta}{\partial n}=K_s\frac{\partial\theta}{\partial n} \tag{6}$$

where K_f and K_s are thermal conductivities of fluid and solid, respectively, and n represents the normal distance.

The governing equations are converted into the non-dimensional form by defining the following non-dimensional variables:

$$X=\frac{x}{L},\quad Y=\frac{y}{L},\quad \zeta=\frac{\omega L^2}{\alpha},\ \psi=\frac{\Psi}{\alpha},\ \theta=\frac{T-T_c}{T_h-T_c},$$
$$\mathrm{Pr}=\frac{\nu}{\alpha},\quad \mathrm{Ra}=\frac{g\beta(T_h-T_c)L^3}{\alpha\nu} \tag{7}$$

The equations (1), (2), (3), and (5) are subjected to the following boundary conditions:

- the lateral walls $X = 0$ and $X = 1$: $\partial\theta/\partial X = 0$,
- the lower wall $Y = 0$: $\theta = 1$,
- the top wall $Y = 1$: $\theta = 0$,
- for all surface walls: $\psi = 0$, and
- for all surface walls: $\zeta 0 = (3/\Delta n^2)(\psi_0 - \psi_1) + \zeta_1/2$ – this formula is known as the Woods condition [25].

The local Nusselt number was defined as:

$$\mathrm{Nu}=\left.\frac{\partial\theta}{\partial N}\right|_w \tag{8}$$

The average Nusselt number was calculated along all area of heated walls according to the equation:

$$\overline{\mathrm{Nu}}=\frac{1}{L+6h}\int_0^{L+6h}\left.\frac{\partial\theta}{\partial N}\right|_w \mathrm{d}s \tag{9}$$

Numerical solution

The governing equations (1), (2), (3), and (5) are solved by finite difference scheme which used central differencing for the second order derivative and upwind or one-sided differencing for non-linear first order convective terms. The role of upwind differencing procedure in stabilizing the numerical scheme has been well documented. The application of this scheme to free convection flow at high Rayleigh number is discussed in [25].

The following is the procedure in [25], the governing finite difference equations for ζ, θ, and ψ can be written in the standard five point formula form. These finite differential equations subjected to appropriate boundary conditions, are solved by an iterative method known as successive substitution. If ζ^s, θ^s, and ψ^s denote functional values at the end of s-th iteration, the values of ζ, θ, and ψ at (s + 1)th iteration level are calculated from the following expressions:

– for vorticity

$$\zeta_{i,j}^{s+1} = (1-\gamma_\zeta)\zeta_{i,j}^{s} + \frac{\gamma_\zeta}{A_\zeta}[a_\zeta \zeta_{i+1,j}^{s} + b_\zeta \zeta_{i-1,j}^{s+1} + c_\zeta \zeta_{i,j+1}^{s} + d_\zeta \zeta_{i,j-1}^{s+1} + 0.5\mathrm{Ra}\,\mathrm{Pr}\,h(\theta_{i+1,j}^{s+1} - \theta_{i-1,j}^{s+1})]$$

– for temperature

$$\theta_{i,j}^{s+1} = (1-\gamma_\theta)\theta_{i,j}^{s} + \frac{\gamma_\theta}{A_\theta}(a_\theta \theta_{i+1,j}^{s} + b_\theta \theta_{i-1,j}^{s+1} + c_\theta \theta_{i,j}^{s} + d_\theta \theta_{i,j-1}^{s+1})$$

– for stream function (10)

$$\psi_{i,j}^{s+1} = (1-\gamma_\psi)\psi_{i,j}^{s+1} + \frac{\gamma_\psi}{4}(\psi_{i+1,j}^{s} + \psi_{i-1,j}^{s+1} + \psi_{i,j+1}^{s} + \psi_{i,j-1}^{s+1} + h^2\omega_{i,j}^{s+1})$$

– for temperature in solid wall

$$\theta_{i,j}^{s+1} = (1-\gamma_{\theta so})\theta_{i,j}^{s+1} + \frac{\gamma_{\theta so}}{4}(\theta_{i+1,j}^{s} + \theta_{i-1,j}^{s+1} + \theta_{i,j+1}^{s} + \theta_{i,j-1}^{s+1})$$

where h is the step size and γ_ζ, γ_θ, γ_ψ, and $\gamma_{\theta \mathrm{so}}$ are overall relaxation parameter which depends on the mesh size and fluid mechanical parameters, and a_ζ, b_ζ, c_ζ, d_ζ, a_θ, b_θ, c_θ, and d_θ are given in [25].

For the interface region, the eq. (6) is solved forward or backward according to the location of the partition. The final form of eq. (6) is:

$$\theta_{\mathrm{int}} = \frac{K_\mathrm{r}\,\theta_\mathrm{f} + \theta_\mathrm{s}}{1 + K_\mathrm{r}} \tag{11}$$

The converged solution was defined to meet the following criterion for all dependent variables:

$$\max.\left|\varphi^{n+1} - \varphi^{n}\right| \le 10^{-4} \tag{12}$$

Model testing

The first stage of data reliability check has been carried out on the basis of the classical problem on free convection in a square cavity with heated lateral walls. Comparison with the standard data of Davis [26] proves results discrepancy, which does not exceed 0.7% for computational grid knots of 80 × 80 in the range of Rayleigh numbers Ra = 10^3-10^6.

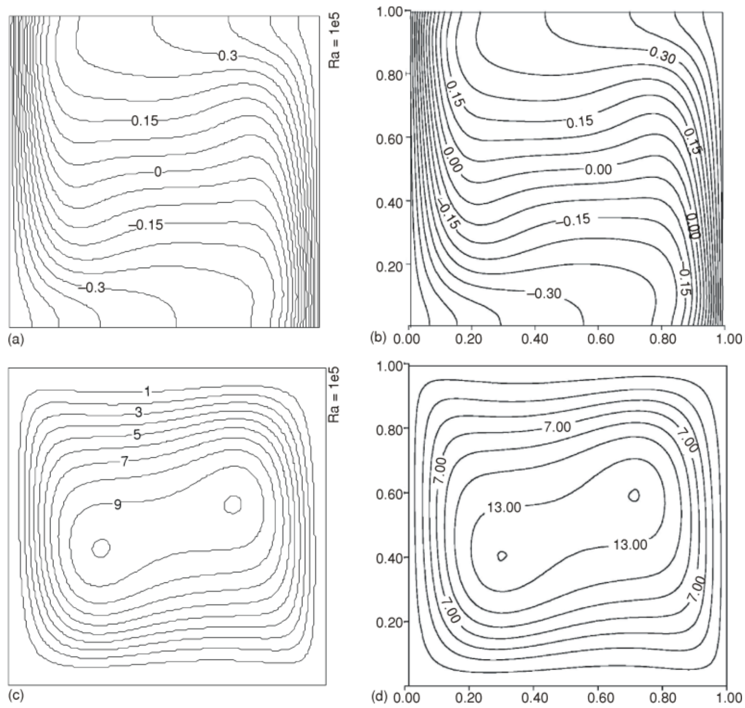

Figure 2. Comparison of isotherms and streamlines for present study (a, c) and isotherms and streamlines from ref. [2] (b, d)

Application of the finer grid did not effect the local and integral characteristics of the flow and heat transfer.

The cavity with partitions was calculated using the finer uniform grid of 120 × ×120 cells. Calculation results were compared with data of [2], where studied geometry of cavity with partitions was the same as in the current study, but the vertical walls were heated and the horizontal ones were adiabatic.

Comparison results are shown in figs. 2 and 3. According to these figures, distributions of isotherms, figs. 2(a), and (b) and streamlines, figs. 2(c) and (d), repeat each other with high accuracy, demonstrating all typical features of fluid motion and thermal structure inside the cavity. Results on integral heat transfer within an interlayer also coincide with data of [2]. This comparison is shown in fig. 3; according to this comparison, with a rise of Ra number the difference in calculation increases, but this value does not exceed ~7%.

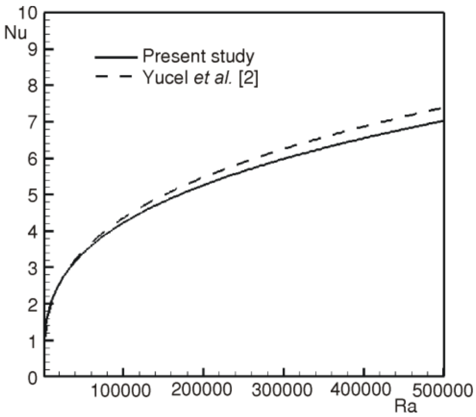

Figure 3. Comparison of data on average heat transfer in cavity with partitions and heated lateral walls

Calculation results and discussion

Streamlines and temperature fields in cavity

The gas flow and heat transfer in partially separated square cavities were studied numerically in the current work. It is assumed that the vertical walls of cavity are adiabatic, and the upper and lower walls are kept at constant, but with different temperatures. The working medium in cavity is air, therefore, Prandtl number is Pr = 0.72. Staggered partitions are placed on both horizontal surfaces (fig. 1). Dimensionless values of partition height were varied in the wide ranges and equaled h/L = 0.0, 0.1, 0.2, 0.3, and 0.4. Their thickness d/L was constant and equal to = 0.1. The position of partitions w_i/L in calculations was not changed also, and values were taken as 0.15, 0.45, 0.75, 0.3, 0.6, and 0.9, respectively.

The relative coefficient of partition heat conductivity was K_r = 2, 5, 10, 20, 50, 100, 1000, and 8000. This range covered the whole set of materials from low-heat-conductive (adiabatic, K_r = 2) to high-heat-conductive (K_r > 1000). Calculations were carried out at different values of Ra = 10^3 to 10^6. To study the flow structure and heat transfer, the streamlines and isotherm behavior in the gas phase and in solid partitions were analyzed and local and average Nusselt numbers were calculated.

Figure 4 illustrates distributions of streamlines and temperature fields for Rayleigh numbers Ra = 10^5 and 10^6 (upper and lower groups of figures, respectively) and for high heat conductivity of partition material K_r = 8000. At low partitions the flow has the form of two--cell vortex, close to the symmetrical one. It is formed by raising forces from the heated surface in the cavity center. With a rise of partition, height symmetry is broken, and the multicell flow is formed in space between the lower and upper partitions. The intensive vortex

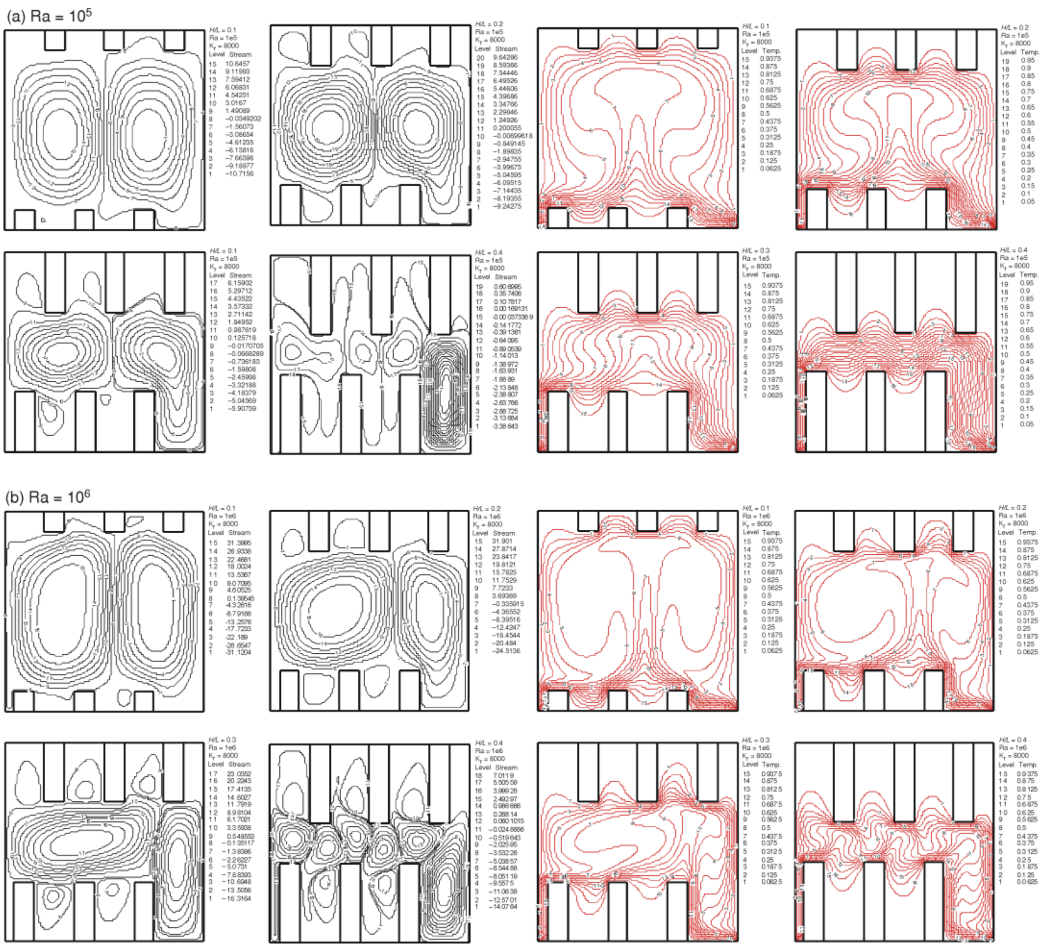

Figure 4. Stream function (two left columns) and isotherms (two right columns) for *h/L* = 0.1, 0.2, 0.3, and 0.4, (a) Ra = 10^5, (b) Ra = 10^6; K_r = 8000

flow, which leads to local enhancement of heat transfer, is observed near the lower heated surface in non-encumbered area. More over, it is necessary to note that the presence of partitions suppresses convective gas motion and stagnation zones are formed in-between the partitions, where it becomes a reason for heat transfer deterioration. For high partitions (h/L = = 0.4) this effect is most obvious.

With a rise of Rayleigh number (Ra = 10^6, fig. 4b) all the above tendencies are kept with the only difference that a loss of flow symmetry is achieved at lower height of partitions. The multicellular structure in the center is the most obvious, and convective cells penetrate deeper into the space in-between the partitions.

The effect of relative heat conductivity coefficient of partition material K_r on stream functions and isotherms is shown in fig. 5. Calculation data for two Rayleigh numbers Ra = = 10^5 and 10^6 are shown there at constant height of partitions h/L = 0.2. It is obvious that with an increase in heat conductivity the circulation cells are formed more intensely in-between the partitions. There are no separated bubbles in the case of adiabatic partitions (K_r = 2.). The

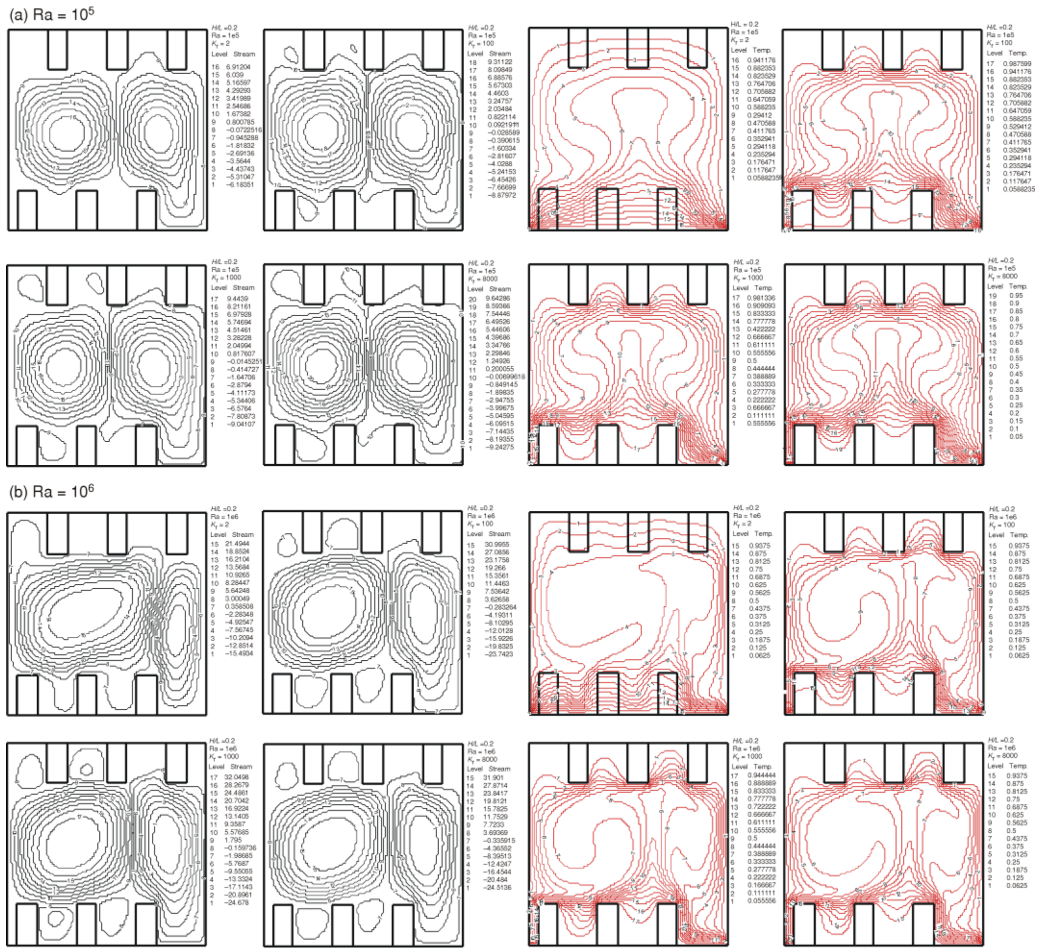

Figure 5. Stream function (two left columns) and isotherms (two right columns) for varying relative heat conductivity K_r: 2, 100, 1000, and 8000 , at (a) Ra =10^5, (b) Ra =10^6 , and h/L = 0.2

weak effect of partitions on heat transfer in this case is proved by isotherm behavior. The influence mechanism of partition heat conductivity on the flow and heat transfer is determined by specific character of zone formation between the partitions. At low heat conductivity there is the high temperature gradient along the surface of the inter-partition cell. For heat conducting partitions this gradient becomes significantly lower, what additionally increases a contribution of raising forces in heat transfer intensification. With a rise of Rayleigh number (fig. 5b) these effects become stronger. With increasing K_r value, the temperature gradient in the partitions diminishes due to high conductivity of partitions.

Local heat transfer

Distribution of local Nusselt number along the outline of the lower heated wall, including the partitions, is shown in fig. 6. Calculation results for different partition height and Relay number are also presented there. For low partitions, fig. 6(a), maximal heat transfer is achieved on the cavity boundaries, where strong descending flows of cold gas occur. In the central part heat transfer is decreased, and in the center, where a thermal vortex is formed, the Nusslet number is close to zero. With a rise of partition height, figs. 6(b) and (d), when partitions start participating in heat transfer, distribution of coefficient becomes absolutely different. On the crest of the partitions at corner points the Nusselt numbers are maximal. In-between the partitions heat transfer decreases drastically, and for highest h/L = 0.4, fig. 6(d), it is zero. At this, heat transfer intensity on the limiting boundaries of cavity decreases also.

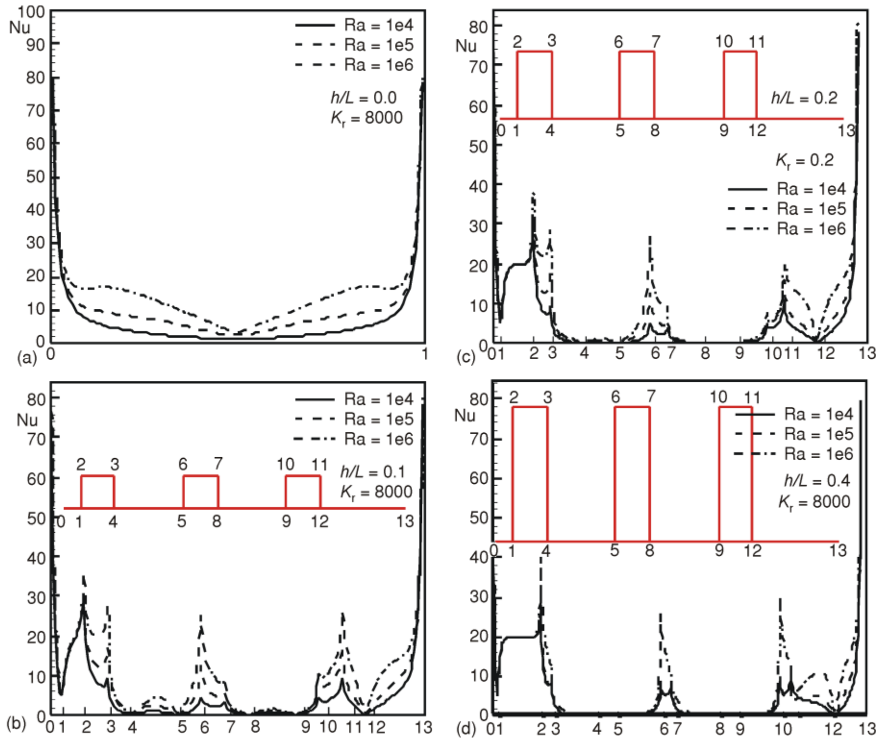

Figure 6. Distribution of local Nusselt number for (a) *h/L* = 0.0, (b) *h/L* = 0.1, (c) *h/L*= 0.2, and (d) *h/L* = 0.4; and Ra=10^4, 10^5, and 10^6; and K_r = 8000

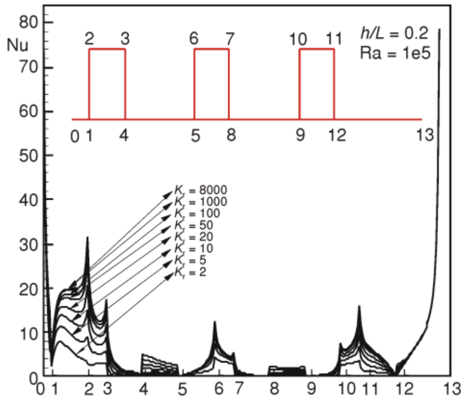

Figure 7. The effect of heat conductivity of partitions on Nusselt number for Ra = 10^5 and h/L = 0.2

The effect of partition heat conductivity on a change in local Nusselt number is shown in fig. 7. As it was expected, for partitions with high heat conductivity, local heat transfer increases. Variation of local Nusselt number shows similar trends for all K_r values.

The effect of partitions on average heat transfer coefficient

The average heat transfer coefficient was calculated by formula (9) along the outline of the heat-exchanging wall and, hence, it related to the whole length of separation line between the gas medium and solid surface. This processing did not consider the development of heat-exchanging surface at the expense of partitions and the effect of this factor on total heat transfer. Results of this processing are shown in fig. 8. Heat transfer decreases with a rise of partition height both for low and high heat conductivity of partitions. This indicates that partition mounting suppresses convective

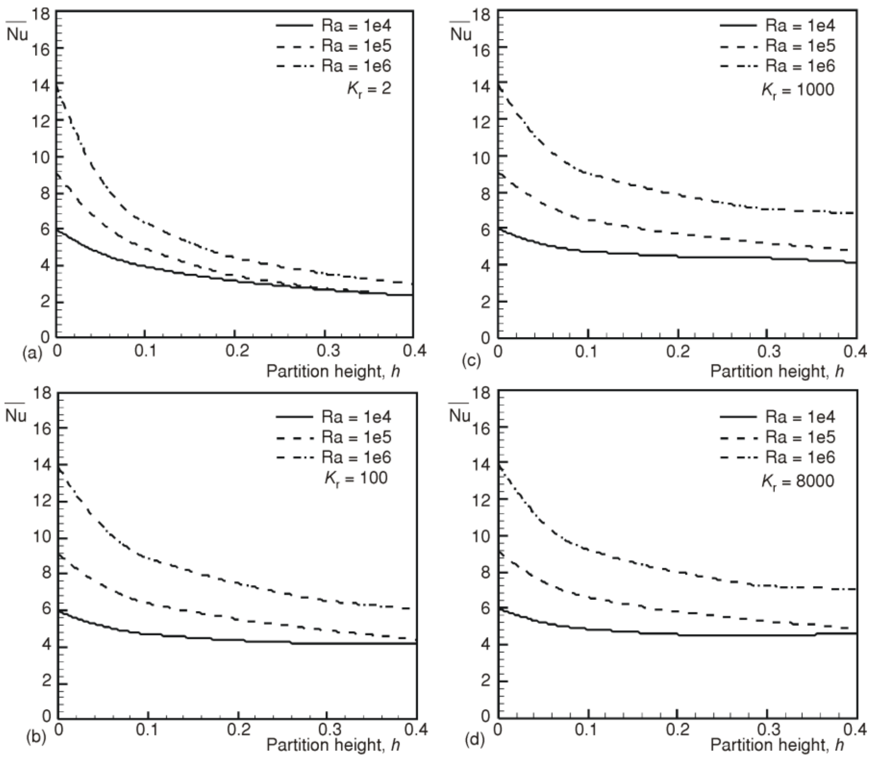

Figure 8. Change in average Nusselt number with a rise of partition height for (a) K_r = 2, (b) K_r = 100, (c) K_r = 1000, (d) K_r = 8000; and Ra = 10^4, 10^5, and 10^6

heat transfer due to breakdown of large convective cells. This agrees absolutely with the conclusions of [2, 3, 8, 9], where reduction of heat transfer intensity at partition mounting was determined. There is a big difference in average Nusselt number without partition for the considered Rayleigh numbers, when the partition height is increased the difference in average Nusselt number for the considered Rayleigh numbers decreases. With the increase of partition height the average Nusselt number seems to reach an asymptotic value. It is necessary to note that with a rise of coefficient K_r the effects of suppression become weaker, what is shown in fig. 9. These effects are relatively low. This is proved by data in fig. 10, where a change in average Nusselt number is shown depending on relative heat conductivity coefficient K_r. Thus, at a change in K_r by four orders, Nusselt number for the highest interlayer changes by the factor of 1.5-2 only.

When analyzing heat transfer in cavities with conducting partitions, it is necessary to take into account that integral heat transfer from the lower to the upper wall depends also on the degree of surface development. With a rise of partition height, the area of heat-exchanging surface increases also. To determine total heat transfer data on average Nusselt number in figs. 9 and 10 should be multiplied by the ratio of developed surface area to the area of similar surface without partitions. It is apparent that in this case dependence of integral heat transfer on the partition height changes absolutely, and with its rise heat transfer increases. This is also proved by calculation results shown in [8, 9].

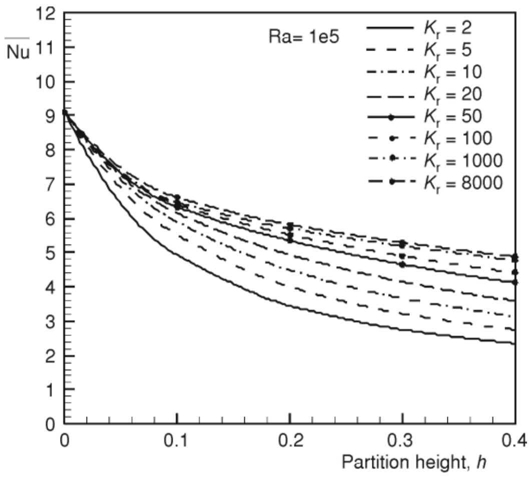

Figure 9. Change in average Nusselt number depending on partition height

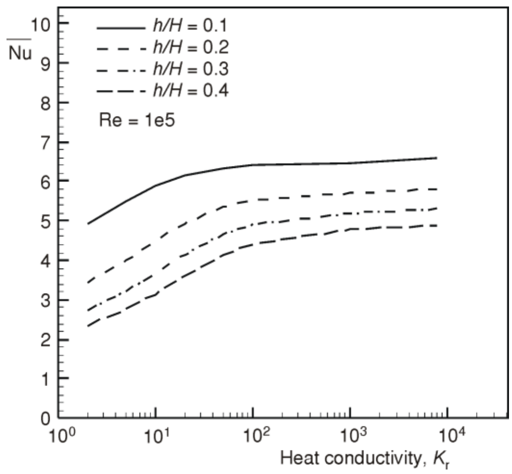

Figure 10. The effect of heat conductivity coefficient on average Nusselt number

The important question in the engineering approach is the definition of integrated heat transfer through all an enclosure. Results of calculations as relation $\overline{\overline{\text{Nu}}}/\overline{\text{Nu}}_0$ are shown in fig. 11 for two Rayleigh numbers Ra = 10^4, fig. 11(a), and Ra = 10^5, fig. 11(b). Here Nu_m is the integrated Nusselt number at the presence of partitions, and $\text{Nu}_{\text{m}0}$ is the Nusselt number at their absence. This kind of calculation results show directly the influence of partition heights and their heat conductivities on an augmentation or suppression of heat transfer.

As compared with fig. 9, where intensity of heat transfer was reduced in the process of an increase in height of ribs, integrated heat transfer in conformity with data in fig.11 grows. Heat transfer increases in all the cases because of an increase in the area of ribs.

Exception is made only by low conductivity ribs and intensive convection inside a cavity, fig. 11(b), $K_r = 2$. Under these conditions of ribbing this results in suppression of heat transfer and $\overline{\overline{\mathrm{Nu}}}/\overline{\mathrm{Nu}}_0 < 1$. It is obvious that this effect will be amplified with a growth of Rayleigh number. Heat conductivity of rib material can change the intensity of heat transfer more than in 2 times. The data in fig. 11 allow us to make an estimation of intensity of total heat transfer through a enclosure at variation of geometrical parameters, rib material, and Rayleigh number.

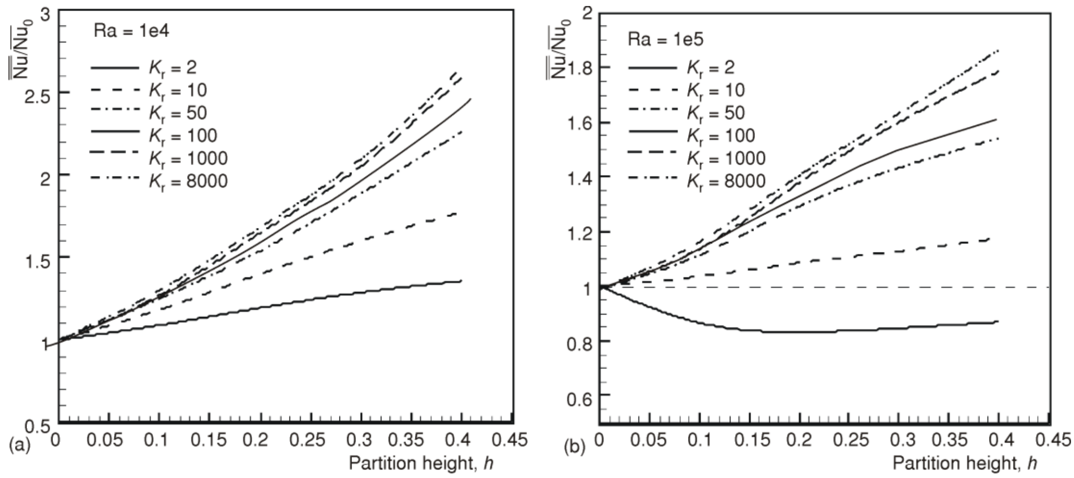

Figure 11. Control of heat transfer through an enclosure due to change of heat conductivity of ribs and their height, for (a) Ra = 10^4 and (b) Ra = 10^5

Conclusions

The numerical model for calculation of free-convective laminar flow and heat transfer in a square 2-D cavity with heated bottom, cooled ceiling, and alternate partitions was developed. The partitions height and their heat conductivity were varied in the wide limits. The model was tested in detail on the classical results available in publications.

The strong effect of partitions on the flow structure and temperature distribution in an enclosure was determined. With a rise of partition height, the symmetrical two-cell flow generated by a thermal vortex in the cavity center turns gradually in the multicellular vortex structure. For the higher Relay numbers symmetry breakdown occurs at lower partitions. For high-heat-conductive partitions flow destabilization occurs at their lower heights.

The presence of partitions affects significantly the regularities of local heat transfer. There are the maximums in distributions of Nusselt number caused by the influence of the edge effects in the corner zones of ribbing elements. In space between the partitions heat transfer decreases significantly, especially for extended partitions and high heat-conductivity coefficients because of formation of poorly blown stagnation zones.

The surface-average heat transfer coefficient decreases with a rise of partition height because of suppression of convection by these partitions. With an increase in heat-conductivity coefficient the Nusselt number in cavity becomes significantly higher. Thus, at a change in the value of relative heat-conductivity coefficient almost by four orders, the

Nu number for the highest partitions changes by the factor of 1.5-2 only. Total heat transfer in the cavity becomes higher due to an increase in the heat exchange area.

Acknowledgment

The work was financially supported by the Russian Foundation for Basic Research (project No. 10-08-00105-a).

Nomenclature

A	–	factor of a cavity expansion, (= H/L), [–]
a	–	thermal diffusivity of fluid, [$\mathrm{m^2s^{-1}}$]
d	–	thickness of the partition, [m]
g	–	gravitational acceleration, [$\mathrm{ms^{-2}}$]
h	–	partition height, [m]
H	–	cavity height, [m]
k	–	thermal conductivity, [$\mathrm{Wm^{-1}K^{-1}}$]
K_r	–	thermal conductivity ratio (= $K_\mathrm{s}/K_\mathrm{f}$), [–]
L	–	length of the cavity, [m]
n	–	normal distance, [–]
Nu	–	local Nusselt number, [–]
$\overline{\mathrm{Nu}}$	–	average Nusselt number, [–]
$\overline{\overline{\mathrm{Nu}}}$	–	average Nusselt number between bottom and top surface, (= $\overline{\mathrm{Nu}}(1 + 6h/L)$), [–]
$\overline{\mathrm{Nu}}_0$	–	average Nusselt number without partitions [–]
Pr	–	Prandtl number (= $\nu_\mathrm{f}/\alpha_\mathrm{f}$), [–]
Ra	–	Rayleigh number (= $\mathrm{g}\beta(T_\mathrm{H} - T_\mathrm{C})L^3/\nu_\mathrm{f}\alpha_\mathrm{f}$), [–]
T	–	temperature, [K]
U	–	dimensionless velocity component in X-direction, [–]
V	–	dimensionless velocity component in Y-direction, [–]
$W_{1\text{-}6}$	–	distance from side wall to partition, [m]
X	–	dimensionless horizontal axis (= x/L), [–]
x	–	horizontal axis, [m]
Y	–	dimensionless vertical axis (= y/L), [–]
y	–	vertical axis, [m]

Greek symbols

α	–	heat transfer coefficient, [$\mathrm{Wm^{-2}K^{-1}}$]
β	–	thermal expansion coefficient, [$\mathrm{K^{-1}}$]
ν	–	kinematic viscosity, [$\mathrm{m^2s^{-1}}$]
θ	–	dimensionless temperature, [–]
ψ	–	stream function, [–]
Ψ	–	dimensionless stream function
ζ	–	dimensionless vorticity

Subscripts

c	–	cold wall
h	–	hot wall
f	–	fluid
s	–	partition (solid)

References

[1] Karayiannis, T. G., Ciofalo, M., Barbaro, G., On Natural Convection in a Single and Two Zone Rectangular Enclosure, *Int. J. Heat Mass Transfer*, *35* (1992), 7, pp.1645-1657

[2] Yucel, N., Ozdem, A.H., Natural Convection in Partially Divided Square Enclosures, *Heat and Mass Transfer*, *40* (2003), 1-2, pp. 167-175

[3] Dagtekin I., Oztop H. F., Natural Convection Heat Transfer by Heated Partitions within Enclosure, *Int. J. Heat Mass Transfer*, *28* (2001), 6, pp. 823-834

[4] Nakhi, A. B., Chamkha., A. J. Natural Convection in Inclined Partitioned Enclosures, *Heat Mass Transfer*, *42* (2006), 4, pp. 311-321

[5] Nansteel, M. W., Greif, R., Natural Convection in Undivided and Partially Divided Rectangular Enclosures, *Journal of Heat Transfer*, *103* (1981), 4, pp. 623-629

[6] Nansteel, M. W., Greif, R., An Investigation of Natural Convection in Enclosures with Two- and Three--Dimensional Partitions, *Int. Journal Heat Mass Transfer*, *27* (1984), 4, pp. 561-571

[7] Lakhal, E. K., *et al*., Natural Convection in Inclined Rectangular Enclosures with Perfectly Conducting Fins Attached on the Heated Wall, *Heat and Mass Transfer*, *32* (1997), 5, pp. 365-373

[8] Terekhov, V. I., Terekhov, V. V., Heat Transfer in a High Vertical Enclosure with Multiple Fins Attached to the Wall, *J. Enh. Heat Trans*fer, *15* (2008), 4, pp. 302-312

[9] Terekhov, V. V., Terekhov, V. I., Numerical Investigation of Heat Transfer in Tall Enclosure with Ribbed Walls, *Computational Thermal Sciences*, *2* (2010), 1, pp. 33-42

[10] Tanda, G., Natural Convection Heat Transfer in Vertical Channels with and without Transverse Square Ribs, *Int. J. Heat Mass Transfer*, *40* (1997), 9, pp. 2173-2185
[11] Shi, X., Khodadadi, J., Laminar Natural Convection Heat Transfer in a Differentially Heated Square Cavity Due to a Thin Fin on the Hot Wall, *Trans. ASME, J. Heat Transfer, 125* (2003), 4, pp. 624-634
[12] Yucel, N., Turkoglu, H., Numerical Analysis of Laminar Natural Convection in Enclosures with Fins Attached to an Active Wall, *Heat and Mass Transfer*, *33* (1998), 4, pp. 307-314
[13] Zimmerman, E., Acharyd, S., Free Convection Heat Transfer in a Partially Divided Vertical Enclosure with Conducting End Walls, *Int. J. Heat and Mass Transfer*, *30* (1987), 2, pp. 319-331
[14] Lakhal, E. K., *et al*., Natural Convection in Inclined Rectangular Enclosures with Perfectly Conducting Fins Attached on the Heated Wall, *Heat and Mass Transfer*, *32* (1997), 5, pp. 365-373
[15] Scozia, R., Frederick, R., Natural Convection in Slender Cavities with Multiple Fins Attached to an Active Wall, *Numerical Heat Transfer*, *Part A – Applications*, *20* (1991), 2, pp.127-158
[16] Mushatet, K. S., Turbulent Natural Convection Inside a Square Enclosure with Baffles, *Procedings* 14th International Heat Transfer Conference, 2010, Washington, DC, USA, IHTC-23397
[17] Ben-Nakhi, A., Chamkha, A. J., Natural Convection in Inclined Partitioned Enclosures, *Heat Mass Transfer*, *42* (2006), 4, pp. 311-321
[18] Al Amiri A., Khanafer, K., Pop, I., Buoyancy-Induced Flow and Heat Transfer in a Partially Divided Square Enclosure, *Int. J. Heat Mass Transfer*, *52* (2009), 15-16, pp. 3818-3828
[19] Wu, W., Ching, C. Y., Laminar Natural Convection in a Square Cavity with a Partition on the Heated Vertical Wall, *Experimental Heat Transfer*, *23* (2010), 4, pp. 298-316
[20] Hung, Y. H., Shiau, W. M., Local Steady-State Natural Convection Heat Transfer in Vertical Parallel Plates with a Two-Dimensional Rectangular Rib, *Int. J. Heat Mass Transfer, 31* (1983), 6, pp. 1279-1288
[21] Viswatmula, P., Amin, M. R., Effects of Multiple Obstructions on Natural Convection Heat Transfer in Vertical Channels, *Int. J. Heat Mass Transfer*, *38* (1995), 11, pp. 2039-2046
[22] Terekhov, V. I., Chichindaev, A.V., Ekaid, A. L., Fluid Flow and Heat Transfer in a Partially Divided Square Cavity with Conducting Ribs, *Procedings*, 29th Siberian Thermophysics Seminar (STS-29) – 2010, Novosibirsk, Ryssia, IT SB RAS, Russia
[23] Nada, S. A., Natural Convection Heat Transfer in Horizontal and Vertical Closed Narrow Enclosure with Heated Rectangular Finned Base Plate, *Int. J. Heat Mass Transfer*, *50* (2007), 3-4, pp. 667-679
[24] Sezai, I., Mohamad, A. A., Suppressing Free Convection from a Flat Plate with Poor Conductor Ribs, *Int. J. Heat Mass Transfer*, *42* (1999), 11, pp. 2041-2051
[25] Nogotov, E. F., Applications of Numerical Heat Transfer, Hemisphere Publ. Corp., Washington, D. C., USA, 1978
[26] Davis, D. V. G., Natural Convection of Air in a Square Cavity: a Bench Mark Numerical Solution, *Int. J. Numer. Methods in Fluids*, *3* (1983), 3, pp. 249-264

Paper submitted: January 9, 2011
Paper revised: April 22, 2011
Paper accepted: May 12, 2011